2002

Development of a Technique to Isolate Measurement of Ionic Mobility

Jie Guo
College of William & Mary - Arts & Sciences

DEVELOPMENT OF A TECHNIQUE TO ISOLATE MEASUREMENT OF IONIC MOBILITY

A Thesis

Presented to

The Faculty of the Department of Chemistry

The College of William and Mary in Virginia

In Partial Fulfillment

Of the Requirements for the Degree of

Master of Arts

---

by

Jie Guo

2002

APPROVAL SHEET

This thesis is submitted in partial fulfillment of

The requirements for the degree of

Master of Arts

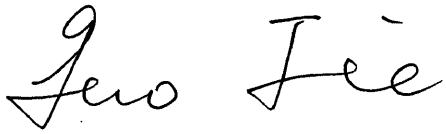

Author

Approved, April 2002

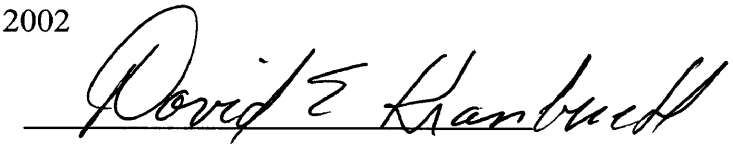

Dr. David E. Kranbuehl

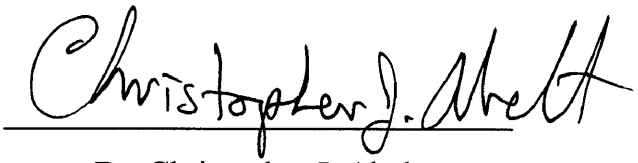

Dr. Christopher J. Abelt

Dr. Robert A. Orwoll

TABLE OF CONTENTS

	Page
Acknowledgements	v
List of Figures	vi
List of Tables	viii
Abstract	ix
Chapter 1.0 Introduction	1
References	5
Chapter 2.0 Time of Flight	7
References	12
Chapter 3.0 Related Experimental Techniques	14
3.1. Frequency Dependent Electromagnetic Sensing	14
3.2. Rheological Measurement	22
3.3. Modulated Temperature Differential Scanning Calorimetry	27
References	29
Chapter 4.0 Experiment Procedure	31
4.1. Experimental Equipments	31
4.1.1. Time of Flight Measurements	31
4.1.2. FDEMS Measurements	32
4.1.3. Rheometry Measurements	33
4.1.4. DSC Measurments	34
4.1.5. Chemical Analytes	35
4.1.6. Sensor Types	38
4.2. Experimental Procedure	39
4.2.1. TOF Experiments	39

4.2.2. FDEMS Experiments 45

4.2.3. Rheometry Experiments 45

References 47

Chapter 5.0 Results and Discussions 48

References 60

Chapter 6.0 Conclusions 61

References 63

VITA 64

ACKNOWLEGEMENTS

The author would like to express her sincere appreciation to Dr. David E Kranbuehl for his invaluable guidance and understanding during this research. The author is also indebted to Dr. Christopher J. Abelt and Dr. Robert A. Orwoll for their contributions to this manuscript and careful instructions during this endeavor.

The author wishes to acknowledge the exceptional support of the Department of Chemistry and all her friends, especially Julie Warner without which her research experience would not have been completed. In particular, thanks are given to Nick Jones, Meisa Khoshbin and all the undergraduate students in Dr. Kranbuehl group.

Finally, the author wishes to express her deepest appreciation to her family for their very generous support. They provided her with encouragement and strength throughout her study.

LIST OF FIGURES

	Page
[Figure 2.1] Equilibrium ion distribution before and at the time of application of the voltage.	7
[Figure 2.2] Scheme of voltage and current time dependencies during the TOF measurement	9
[Figure 3.1] Parallel Plate Capacitor	17
[Figure 3.2] Effect of polarization of (a) ion (b) dipolar rotation	18
[Figure 3.3] Phase Shift between Shear Stress/ Shear Strain	25
[Figure 4.1] TOF Experimental Setup	32
[Figure 4.2] FDEMS Sensor	33
[Figure 4.3] Rheometer Setup (a) Peltier Plate (b) Parallel Plate	34
[Figure 4.4] DSC Experimental Setup	35
[Figure 4.5] Struture of 1,1-bis(4-cyanatophenyl) ethane	36
[Figure 4.6] Structure of epoxy of diglycidylether of bisphenol-A (DGEBA)	37
[Figure 4.7] Structure of polysulfone	37
[Figure 4.8] Structure of o-terphenyl	37
[Figure 4.9] Structure of MCDEA	37
[Figure 4.10] Structure of dimethacrylate of tetaethoxylated bisphenol-A (D121)	38
[Figure 4.11] DGEBA: 25C capacitor 60s 400V	41
[Figure 4.12] D121: 40C capacitor 240s 400V	42
[Figure 4.13] D121: 40C capacitor 15s 50V	43
[Figure 4.14] D121: 40C capacitor 240s 200V	43

[Figure 5.1] DGEBA ln Viscosity vs. (1/T) 48

[Figure 5.2] D121 ln Viscosity vs. (1/T) 49

[Figure 5.3] D121 IDEX Sensor @40C Pulse Length Dependent Data 51

[Figure 5.4] D121 Small Capacitor @40C Pulse Length Dependent Data 52

[Figure 5.5] D121 Small Capacitor Temperature Dependent Data 53

[Figure 5.6] DGEBA Small Capacitor Temperature Dependent Data 54

[Figure 5.7] D121 TOF and FDEMS Sigma verse Temperature 56

[Figure 5.8] D121 IDEX Sensor (TOF*V*Sigma) vs. Temp 57

[Figure 5.9] DGEBA small Capacitor (TOF*V*Sigma) vs. Temp 58

[Figure 5.10] D121 IDEX Sensor Viscosity Dependent Data 59

LIST OF TABLES

	Page
[Table 4.1] Parameters of Sensors	39
[Table 4.2] Tg and TOF Temperature Range	40

ABSTRACT

An appropriate technique, Time of Flight, is proposed and developed to isolate and monitor the mobility of ionic species from the conductivity. Typically the conductivity is measured through dielectric technique, Frequency Dependent Electromagnetic Sensing. Therefore, correlated to FDEMS, TOF measurement is able to provide more accurate information regarding the changing in the species, as well as in the concentration of ions in the physical and chemical states during the curing process.

Presently, there is an assumption in previous reports that the number of charge carriers, N_i, remains constant in a curing material. This is particularly true when approximately relating the electrical conductivity to the macroscopic viscosity. But in the most of case, N_i is not a constant at all. The most prevalent instance is in hydrogen-bonded systems, where proton conduction and free ion proximity cause the changing of number of charge carriers. Time of Flight measurement is a really promising technique, because of its capability of isolating the mobility measurement from the conductivity. Therefore, equipped with dielectric measurement, TOF is powerful to separately monitor changes in the numbers of charge carriers due to temperature alterations in the curing process.

The first step of this research was to develop the Time of Flight technique by optimizing the experimental parameters on a list of pulse length, applied voltage, and temperature. After setting up a stated mode of experiment and data analysis in the simplest non-hydrogen-bonded system, the technique is appropriately applied to the hydrogen-bonding systems where the effects of number and type of H-bonding groups on mobility will be isolated. My research then involved the examination of a hydrogen-bonding system, attempting to compare the different result of the two media in which the TOF measurement is applied. Also supported with the successful experiments of FDEMS and viscosity measurements, the research is able to focus on verification of Time of Flight technique by correlating the relationship of conductivity, mobility, and viscosity of a material due to the temperature alternation.

DEVELOPMENT OF A TECHNIQUE TO

ISOLATE MEASUREMENT OF IONIC MOBILITY

Chapter 1.0

Introduction

The purpose of this research is to develop Time of Flight technique on the basis of previous experiments and then use the technique to separately monitor changes in the number of charge carriers along with changes in mobility of a polymer during a curing process or temperature variations.

In the applied science field, the ability to monitor in situ the process of any physical and chemical state is highly desired. In this research the curing process of a polymer is most interested. The technique of monitoring electrical and material properties throughout the reaction is an appropriate method. Typically the electrical conductivity, σ, is measured through dielectric measurements using an in-situ micro-sensor and a multi-frequency impedance analyzer. The impedance of a material is measured over a range of frequencies, giving the value of capacitance (C) and conductance (G), through the equation

$$Z^{-1} = G + i\omega C$$

[Equation 1.1] [1]

where $\omega = 2\pi f$. Then another quantity ε^*, the complex permittivity of a material, can be determined with a known G and C value by the following equations,

$$\varepsilon^* = \varepsilon' - i\varepsilon''$$

[Equation1.2] [2]

$$\varepsilon' = C / C_o$$

[Equation 1.3]

$$\varepsilon'' = G / \omega C_o$$

[Equation 1.4]

where C_o is the air replaceable capacitance of the sensor. At low viscosities, low frequencies, and high temperature, the ionic conductivity dominates the impedance of a material. In this case,

$$\sigma = \omega \varepsilon_o \varepsilon''$$

[Equation 1.5] [3]

where ε_o is the permittivity of free space equal to $8.854 \times 10^{-14} C^2 J^{-1} cm^{-1}$.

The ionic conductivity of a material on a molecular level is the sum of the product of the number of ions and their respective mobility,

$$\sigma = \sum N_i \mu_i$$

[Equation 1.6] [4]

where μ is the translation mobility of ions, and N is the number of ions of that species. In general, an inverse proportionality between viscosity and ionic conductivity is observed as previously reported. [5-8]

$$\sigma = k \eta^{-x}$$

[Equation 1.7] [4]

where η is viscosity, a macroscopic characteristic, k is a constant, and x is a value between 1 and 0. Previously reported studies applied the in-situ measurement of σ to

monitor viscosity, which is impossible to be monitored directly and on-line during cure. But certainly only where the number of ions remains constant is the assumption equating conductivity to ionic mobility valid. For a general understanding of electrical mobility related to the macroscopic viscosity, this assumption could be accurate. But in the most of case it could lead to inaccuracies in measurements of viscosity from conductivity, where the number of ions, N_i, is no longer a constant any more. In hydrogen-bonded systems, proton conduction and free ion proximity cause a changing number of charge carriers. Epoxies, polyamides and polyimides are widely used polymer system in industries, and are examples of materials that do not have a constant number of ions.

Appropriate techniques that could isolate the number of ions from their mobility will be valuable in accurate monitoring changes in the physical and chemical state during cure process. Time of Flight measurement is a powerful, promising technique to isolate and measure ionic mobility. Correlated to dielectric measurement of conductivity, the Time of Flight technique will permit separate measurement of changes in the number of mobile ions along with changes in ionic mobility of a polymer system throughout the curing process.

Since the Time of Flight technique is a new technique for this application, there are several variables that affect the measurement result. The primary goal of this research is to develop the appropriate parameters of this technique over a range of temperature, length of voltage pulse, magnitude of applied voltage, and viscosity. As

in previous reports, the Time of Flight technique was used at a fixed voltage and pulse length.[9,10] But in this research, because materials experience significant changes in viscosity during temperature variation, the pulse length and voltage should be adjusted to obtain accurate data. Two types of polymer systems were examined in the research, the non-hydrogen-bonded model and hydrogen-bonded model. Due to the simplicity of the non-hydrogen-bonded model, it was more focused on than hydrogen-bonded model. Consequently most of the discussion and conclusions resulted from the non-hydrogen-bonded system. Further studies will concentrate on model H-bonded systems to relate proton mobility to structure, type and proximity of proton donation groups, particularly in epoxy resins.

Reference for Chapter 1.0

1. Jonscher, A.K. Dielectric Relaxation in Solids, Chelsea Dielectrics Press, London, 1983.
2. Chelkowski, A. Dielectric Physics, Elsevier Scientific Publishing Company, New York, 1980.
3. Kranbuehl, David E. "Dielectric Monitoring of Polymerization and Cure." In Dielectric Spectroscopy of Polymeric Materials, Runt, J.P., Fitzgerald, J.J., Eds., American Chemical Society, Washington, DC, 1997, Chapter 11.
4. Seanor, Donald A. "Electrical Conduction in Polymers." In Electrical Properties of Polymers, Academic Press, Inc, New York, 1982.
5. Koike, T. " Determination of Glass Transition Temperature from Viscosity and Conductivity Measurements for an Epoxy-Amine System During Curing" J. Appl. Polym. Sci. 50, 1993.
6. Maistros, G., Block, H., Bucknall, C., and Partridge, I. "Dielectric Monitoring of Phase Separation during Cure of Blends of Epoxy Resin with Carboxyl-terminated poly (butadiene-co-acrylonitrile)" Polymer, 33, 1992.
7. Simpson, J., and Bidstrup, S. " Rheological and Dielectric Changes Druing Isothermal Epoxy-Amine Cure" J. Polym. Sci. Polym. Phys., 33, 1995.
8. Simpson, J., and Bidstrup, S. " Correlation Between Chin Segment and Ion Mobility in an Epoxy Resin System" J. Polym. Sci. Polym. Phys., 31, 1993.

9. Ulanski, F., Friedrich, K., Boiteux, G., Seytre, G., "Evolution of Ion Mobility in Cured Epoxy-Amine System determined by Time-of-Flight Method" Journal of Applied Polymer Science, 65, 1997.

10. Tournilhac, F, Bassoul, P., Barnik, M., Blinov, L. "Transient Current Measurements in Molecular Materials: Novel Procedure for the Data Treatment" Molecular Materials, 9, 1998.

Chapter 2.0

Time of Flight

Time of Flight is a powerful, promising technique to measure charge transport. By this technique, it is possible to study the transit time of charge carriers directly across a fixed distance between electrodes. Therefore, charge carrier mobility, and so-called ionic mobility can be measured separately from conductivity, which is generally measured through dielectric spectroscopy.

Typically, ionic mobility is examined as a function of conductivity, and concentration of the ions is assumed to be constant. The equation expressing this relation is described as

$$\sigma=\sum N_i \mu_i$$

[Equation 2.1] [1]

Where, σ represents conductivity, Ni is the number of ith ion species and represents the ion concentration in solution, and μ_i is the translation mobility of that ion.

Because our measurements systems are in a liquid state, a simple model for an ionic conductor with blocking electrodes is described in [Figure2.1] [2].

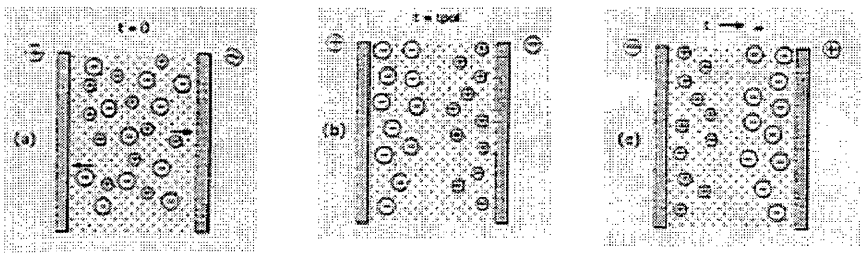

[Figure 2.1] a) Equilibrium ion distribution before and at the time of application of the voltage

b) Steady-state ion distribution at the end of first poling process, $t=t_{pol}$.

c) The ion distribution at the end of second depolarization process, $t=\infty$.

TOF technique uses these two poling steps. The first step creates the polarization of charge at the electrodes. The second step involves measuring the time for this concentration of charge to move to the opposite electrode after reversing the voltage. In the second step, TOF uses the shape of current versus time after a reversal of the voltage polarity to find a characteristic maximum value of the curve. This time marks the transit time of carrier between electrodes.[3]

When first applied, the voltage at the electrodes results in an attraction between opposite charges, and the anions move towards the anode, while cations migrate towards the cathode. After a certain amount of time, long enough to accumulate mobile ions in the vicinity of the electrodes, the polarity of applied voltage is reversed. Then these ions are drawn to the opposite electrode. The number of ions reaching the electrodes produces the output current. Thus the current is a function of concentration of mobile ions. A peak in the current occurs when the ions, which were pulled to the electrodes in step 1, have moved across the distance separating the electrodes during the voltage reversal step. After a time, an accumulating process leads to a decrease of the mobile ion concentration, and consequently, to a decrease of this ion diffusion current.[3] Due to the voltage being applied in consecutive voltage pulses, the observed current after the initial polarization pulse is in the form of a series

of humps. Figure 2 depicts the voltage cycle used for the TOF measurements, with corresponding current signals during a four-pulse sequence.

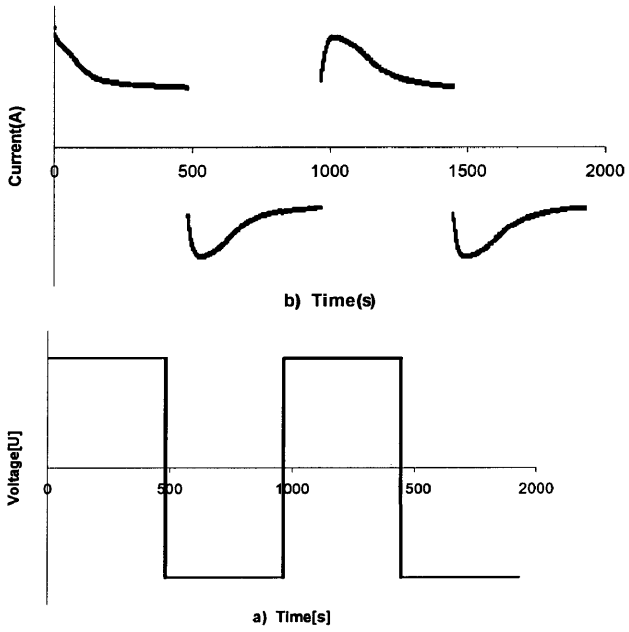

[Figure 2.2] Scheme of a) voltage and

b) Current time dependencies during the TOF measurement

TOF records two observed quantities: 1. transit time, or time-of-flight T (T), which equals the time interval between t_{peak} and t_o ; 2. equilibrium current (I), the current at the end of the pulse. A simple relation can be deduced from the following derivations

$$T = d / v_d$$

[Equation 2.2] [1]

Where, d is the distance between two electrodes, v_d is the drift velocity.

Assuming that average electric field E in the sample is not significantly impacted by the accumulated charge, then

$$E = V / d$$

[Equation 2.3]

where V is applied voltage. The relation between ion mobility and drift velocity is

$$v_d = \mu E$$

[Equation 2.4]

where μ is ion mobility. Combining the equations 2,3,4, the result is

$$\mu = d^2 / TV$$

[Equation 2.5]

Equation 2.5 describes how the effective ion mobility can be calculated through measurement of T and the fixed parameters V and d.

In a polymer system, viscosity and ion conductivity are macroscopic measurements governed by microscopic properties. They characterize chain segment mobility and ion mobility.[3] In general, an inverse proportionality between viscosity and ionic conductivity is observed as previously reported. [4-7]

$$\sigma = k \eta^{-x}$$

[Equation 2.6] [1]

Where η is viscosity, k is a constant, and x is a value between 1 and 0.

Substituting equation 2.6 into equation 2.1, and assuming N is constant, an equation is derived in which ionic mobility is directly related to viscosity

$$\mu = K/ \eta^{x}$$

[Equation 2.7]

Where K is a fitting constant.

As described in the above equations, the following factors affect time-of-flight time T: the magnitude of the applied voltage, length of time of the pulse, the distance between the two electrodes (sensor geometry), and the viscosity of the medium. The amount of mobile charge present in the dielectric medium should be insufficient to perturb the applied electric field.[1] The applied voltage should be strong enough to make certain that all of the ions travel the distance between the electrodes. Furthermore, the pulse length should be long enough to bring the ions to the electrodes. If the pulse length is too small, some of ions are left "floating" between the electrodes.[8] In this case the observed transit time of the polarized charge will be shorter than the true time as many ions have not completed the total distance.

References for Chapter 2.0

1. Seanor, Donald A. "Electrical Conduction in Polymers." In Electrical Properties of Polymers, Academic Press, Inc, New York, 1982.
2. Tournilhac, F, Bassoul, P., Barnik, M., Blinov, L. "Transient Current Measurements in Molecular Materials: Novel Procedure for the Data Treatment" Molecular Materials, 9, 1998.
3. Ulanski, F., Friedrich, K., Boiteux, G., Seytre, G. "Evolution of Ion Mobility in Cured Epoxy-Amine System determined by Time-of-Flight Method" J.Appl.Polym.Sci, 65, 1997.
4. Koike, T. " Determination of Glass Transition Temperature from Viscosity and Conductivity Measurements for an Epoxy-Amine System During Curing" J. Appl. Polym. Sci. 50, 1993.
5. Maistros, G., Block, H., Bucknall, C., and Partridge, I. "Dielectric Monitoring of Phase Separation during Cure of Blends of Epoxy Resin with Carboxyl-terminated poly (butadiene-co-acrylonitrile)" Polymer, 33, 1992.
6. Simpson, J., and Bidstrup, S. " Rheological and Dielectric Changes Druing Isothermal Epoxy-Amine Cure" J. Polym. Sci. Polym. Phys., 33, 1995.
7. Simpson, J., and Bidstrup, S. " Correlation Between Chin Segment and Ion Mobility in an Epoxy Resin System" J. Polym. Sci. Polym. Phys., 31, 1993.
8. Khoshbin, Meisa Silvaine, Bachelor Thesis, College of William & Mary,

Williamsburg, VA 2001.

Chapter 3.0

Related Experimental Techniques

Along with the focus of this work Time of Flight, three related techniques are used in this research: Frequency Dependent Electromagnetic Sensing; Rheological Measurement; and Modulated Temperature Differential Scanning Calorimetry. Conductivity and viscosity measurements were conducted to test and verify relations from Equation 2.1 to Equation 2.7, and DSC measurements were used to estimate the liquid-solid Tg transition temperature of the materials, which served as the lowest temperature of interest for TOF measurements.

3.1. Frequency Dependent Electromagnetic Sensing

FDEMS, Frequency Dependent Electromagnetic Sensing is a versatile, convenient method for measuring microscopic changes in a system which undergoes chemical reactions accompanied by changes in the physical properties such as crystallization, gelation and/or vitrification, phase separation, polymerization, etc. FDEMS employs impedance measurement to monitor motions of ions and dipole particles in the dielectric medium.[1] The measurements are taken in-situ by using a sensor probe. This allows continuous monitoring of advancement of the reaction process in a nondestructive way. A unique characteristic of FDEMS is the wide

frequency range, from the hertz to the megahertz, over which the ions and dipoles in a polymer material respond to an applied electric field.[2]

The foundation of the technique is the ability to monitor at the molecular level, the translation mobility of ions and rotational mobility of dipoles in the presence of a force created by an electric field.[1] FDEMS measurements are useful over periods from a few seconds to numbers of years (life monitoring). Measurements of ionic and dipolar mobility can be used to monitor changes in macroscopic properties, such as viscosity, Tg, and degree of cure of a dielectric material.[3]

Polarization

To better understand FDEMS, one should examine the electrical properties of atoms and molecules in an electric field. Atoms and molecules are electrically neutral, but they contain spatially separated electrical charges under an applied electric field, E.[4] There are three different responses to an applied field E: ions travel to their respective oppositely charged electrode; electron clouds of atoms and molecules distort form their original position; and dipoles rotate to align opposite to the electric field. The response to these last two phenomena is described by polarizability, α_t. The polarizability relates to an average total polarized dipole moment of a molecule, μ_t, by

$$\mu_t = \alpha_t F$$

[Equation 3.1] [5]

where F is the applied internal electric field acting on the molecule.

The three distinct components compose the total polarization in response to E.

$$P_{total} = P_{distortion} + P_{dipolar}$$

[Equation 3.2] [6]

where $P_{distortion}$ is distortion polarization due to the perturbation of the electron cloud surrounding the nucleus and the displacement of the atomic nuclei and results in the rearranging of the atomic bond angels and bond lengths, and $P_{dipolar}$ is the dipolar orientation polarization aroused from rotational dipole movement.

Therefore the total polarization P_{total} is the product of the number of molecules, N, and the total polarized dipole moment per molecule.

$$P_{total} = N \alpha_t F$$

[Equation 3.3] [6]

In the dipolar region of absorbance, by using proper frequencies, FDEMS is effectively able to separate and accurately measure $P_{dipolar}$ from P_{total}, by

$$P_{dipolar} = N \alpha_{dipolar} F$$

[Equation 3.4] [1]

Capacitance

To better understand how FDEMS measurements relate to electrical impedance requires an understanding of capacitance. Capacitance is the ability of a material to store a given charge for a given potential difference.[7] Here we introduce a parallel plate capacitor to illustrate the theory and the relation to the electrical impedance. A fixed distance separates the two identical plates, and each plate is created charge +/- Q on opposite plates, by applied voltage V. [Figure 3.1]

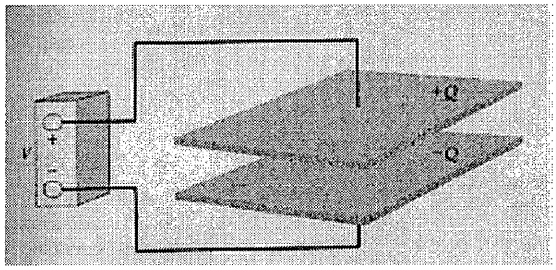

[Figure 3.1] Parallel Plate Capacitor[8]

The capacitance is defined as the ratio of the magnitude of charge, Q and the applied voltage, V

$$C = Q / V$$

[Equation 3.5] [7]

When a dielectric material is put between the two plates, the electric field polarizes the dielectric material, so as to produce charge in the material [Figure 3.2].

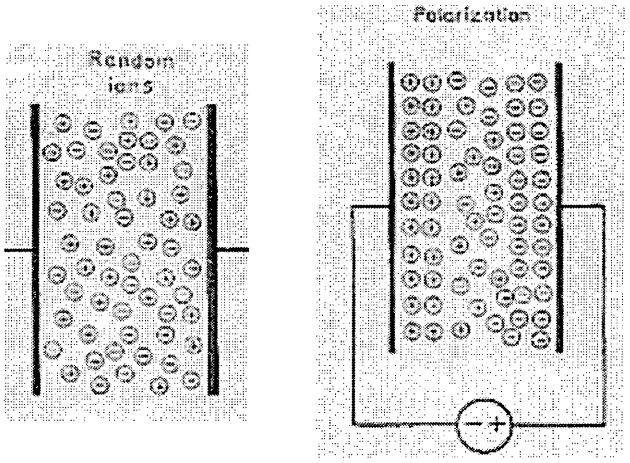

(a)

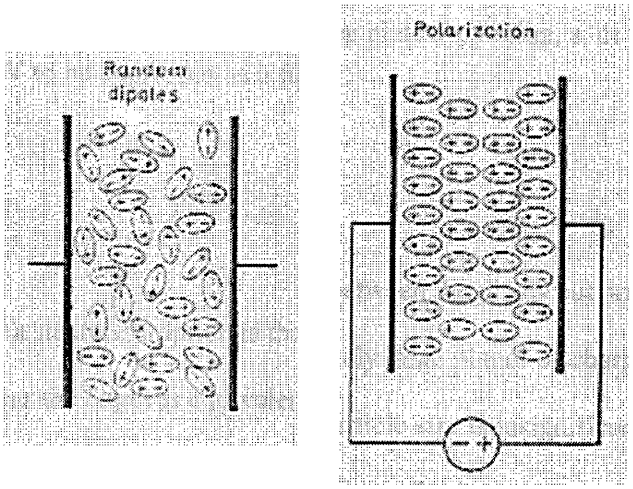

(b)

[Figure 3.2] Effect of polarization of (a) ion (b) dipolar rotation[1]

Correspondingly, the polarization of the dielectric material affects the charge distribution on the two plates, which changes the capacitance

$$C = (Q+P) / V$$

[Equation 3.6] [6]

where P is the polarization of the material.

If the plates are placed close enough to each other, the electric field at any point

between the two plates can be assumed to behave as though the point were next to an infinite plane of change. So the surface charge density, σ, can be defined as the charge per unit area, A

$$\sigma = Q/A$$

[Equation 3.7] [7]

Using Gauss' law, each plate contributes an electric field, E_n, as

$$E_n = \sigma / 2\varepsilon_o$$

[Equation 3.8] [4]

where ε_o is the permittivity of free space equal to $8.854 \times 10^{-14} C^2 J^{-1} cm^{-1}$. When considering two plates, the total field, E_t, is defined as

$$E_t = \sigma / \varepsilon_o$$

[Equation 3.9]

The potential between the plates producing the electric field is

$$V = E_t s$$

[Equation 3.10] [7]

where s is the distance of the two plates. Substituting equation 3.9 into equation 3.10 gives

$$V = \sigma s / \varepsilon_o$$

[Equation 3.11]

Placing equation 3.7 into equation 3.11 leads to

$$V = Qs / A \varepsilon_{\circ}$$

[Equation 3.12]

Then combining equation 3.12 with equation 3.5, the capacitance is finally defined as

$$C = s / A \varepsilon_{\circ}$$

[Equation 3.13] [7]

The last step shows that the capacitance only relies on the geometry of the system used.

Permittivity

Central to FDEMS is the use of impedance measurements, which are frequency dependent. The relation between impedance, conductance and capacitance is

$$Z^{-1} = G + i\omega C$$

[Equation 3.14] [9]

where Z, G, C represent impedance, conductance, and capacitance respectively, ω is the product of 2π and the frequency, and i is the imaginary component. The complex permittivity, ε^*, is related to the dielectric permittivity, ε', and the dielectric loss factor, ε'' by

$$\varepsilon^* = \varepsilon' - i\varepsilon''$$

[Equation 3.15] [10]

The relationship of the complex permittivity to conductance, and capacitance is

defined using the current, I, in amperes, as

$$I = i\omega C_o \varepsilon^* V$$

[Equation 3.16] [10]

Substituting equation 3.15 in equation 3.16 gives

$$I = (i\omega C_o \varepsilon' + \omega C_o \varepsilon'')V$$

[Equation 3.17] [11]

Since Ohm's Law is V=IZ, the following equation can be derived

$$Z\text{-}1 = i\omega C_o \varepsilon' + \omega C_o \varepsilon''$$

[Equation 3.18]

Combining equation 3.18 and equation 3.14 leads to

$$G + i\omega C = i\omega C_o \varepsilon' + \omega C_o \varepsilon''$$

[Equation 3.19]

Then separating the real and imaginary part yields two equations[3]

$$\varepsilon' = C_{material} / C_o$$

[Equation 3.19]

$$\varepsilon'' = G_{material} / \omega C_o$$

[Equation 3.20]

Both ionic and dipolar components contribute to the dielectric permittivity and the dielectric loss factor. Therefore, both ε', and ε'' can be described as[3]

$$\varepsilon' = \varepsilon'_i + \varepsilon'_d$$

[Equation 3.21]

$$\varepsilon'' = \varepsilon''_i + \varepsilon''_d$$

[Equation 3.22]

With the experimental condition varying, either the ionic or dipolar terms may dominate. For instance, during a temperature ramp, at low temperature and high frequencies, where the medium is quite viscous, the dipolar rotation supplies generally higher contributions than the ionic mobility. But at high temperature and low frequencies, where the medium is very fluid, the ionic motion gives a larger response. Considering the combined influence of the ionic and dipolar motion to the dielectric loss factor, gives

$$\varepsilon'' = (\sigma / \omega \varepsilon_o) + [(\varepsilon_o - \varepsilon_\infty) \omega^2\tau] / (1 + \omega^2\tau^2)$$

[Equation 3.23] [1]

By ignoring the second term, the dipolar polarization, which is insignificant at low viscosities and at low frequencies (less than 1000 Hz), equation 3.23 can be reduced to

$$\sigma = \omega \varepsilon_o \varepsilon''$$

[Equation 3.24] [3]

3.2. Rheological Measurement

Rheology is defined as the science of the deformation and flow of matter.[12]

Rheological data give insight into the dynamical and mechanical properties of materials such as viscosity, gel point, and modulus. This research employed a rheometer to acquire viscosity at different temperature. Viscosity is the resistance of a fluid to flow. It results from the movement of any solid object through the fluid, or the motion of the fluid itself past obstacles, or even internally on the fluid between different moving-rate adjacent layers.[13] In general, on a macroscopic scale, the equation describing the relation of viscosity is

$$F/A = \tau = \eta (d\gamma/dt)$$

[Equation 3.25] [14]

where F is a shear force, A is the area, and τ, η, γ are shear stress, viscosity, and strain respectively. Time dependent rheology takes measurements of the sinusoidal stress, τ, (force per unit area) and strain, γ, (change in dimension per unit dimension), and uses this data to gain insight into the viscoelastic properties of the material as a function of frequency. This experiment used a Rheometrics Dynamic Analyzer 1000 to attain the coefficient of viscosity. The rheometer takes measurements by imposing a sinusoidal shear force on the sample. A parallel plate geometry is used in this experiment, and samples are sandwiched between two plates of known distance. The experiment is the so-called constant stress, strain measurement. A motor drives one plate to oscillate, while the other is activated due to a torque transducer, describing the responding strain of the materials. The force and the strain are between 0° to 90° out of phase for viscoelastical materials.[15]

In this type of experiment an oscillatory stress is applied to the sample. The frequency of the oscillation can be varied over an enormous range. The equation describing the applied shear stress is[14]

$$\tau = \tau_o \sin(\omega t)$$

[Equation 3.26]

where ω is the angular frequency of the applied stress in radians/sec (equal to $2\pi f$, where f is the frequency in cycles/sec).

If the sample happens to be perfectly elastic, then the strain would be completely in-phase with applied stress and would vary as

$$\gamma = \gamma_o \sin(\omega t)$$

[Equation 3.27]

But most polymers behave somewhere between totally fluid and perfectly elastic, and so are considered viscoelastic. The resulting strain is out of phase with applied stress with a phase angle of δ, somewhere between 0^o to 90^o. The corrective equation for the resulting strain is given

$$\gamma = \gamma_o \sin(\omega t - \delta)$$

[Equation 3.28]

It is actually more convenient (and usual) to "reset and zero" and consider the stress "leading" the strain by an amount of an angle δ, so that

$$\tau(t) = \tau_o \sin(\omega t + \delta)$$

[Equation 3.29]

and

$$\gamma(t) = \gamma_o \sin(\omega t)$$

[Equation 3.30]

A graph describes the relation of the applied stress and the resulting strain in [Figure 3.3].

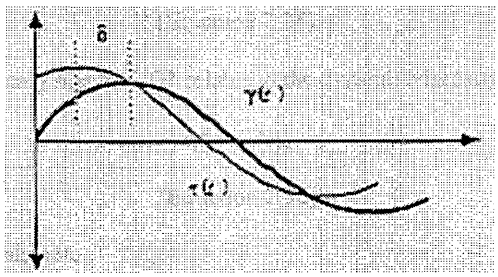

[Figure 3.3] Phase Shift between Shear Stress/ Shear Strain[16]

Equation 3.29 can be rewritten as:

$$\tau(t) = (\tau_o \cos\delta)\sin\omega t + (\tau_o \sin\delta)\cos\omega t$$

[Equation 3.31]

which expresses the stress in terms of an in-phase component ($\sin\omega t$) and an out-of-phase component ($\cos\omega t$) with respect to the strain. By considering Hooke's law

$$\tau(t) = G\ \gamma_o \sin(\omega t)$$

[Equation 3.32]

The relationship between stress and strain can now be defined as

$$\tau(t) = \gamma_o [G'(\omega) \sin \omega t + G''(\omega) \cos \omega t]$$

[Equation 3.33]

The in-phase component, $G'(\omega)$, so-called the storage modulus, and the out-of-phase component, $G''(\omega)$, the loss modulus, are defined individually as

$$G'(\omega) = (\tau_o / \gamma_o) \cos \delta$$

[Equation 3.34]

and

$$G''(\omega) = (\tau_o / \gamma_o) \sin \delta$$

[Equation 3.35]

$G'(\omega)$ and $G''(\omega)$ separately represent the storage of the elastic energy (G') and the dissipation, or loss, of the elastic energy (G''). They combine to create the complex shear modulus, G*, where

$$G^* = G'(\omega) + i\, G''(\omega)$$

[Equation 3.36]

The relationship between the complex shear modulus and the dynamic viscosity, η^*, is

$$\eta^* = G^* / \omega$$

[Equation 3.37] [16]

Equation 3.36 can be rewritten as two terms

$$\eta' = G'(\omega) / \omega \quad \text{and} \quad \eta'' = G''(\omega) / \omega$$

[Equation 3.38] [Equation 3.39]

Substituting G'(ω) and G''(ω) with the previous derivation, gives

$$\eta' = [\ \tau\ (t) \sin(\omega t)/\ \gamma\ (t) \cos(\omega t + \delta)]\ \cos\ \delta\ /\ \omega$$

[Equation 3.40]

and

$$\eta'' = [\ \tau\ (t) \sin(\omega t)/\ \gamma\ (t) \cos(\omega t + \delta)]\ \sin\ \delta\ /\ \omega$$

[Equation 3.41]

Through rheological measurement, a viscosity versus temperature measurement can be attained experimentally. Values of viscosity then are correlated to TOF and FDEMS measurements.

3.3. Modulated Temperature Differential Scanning Calorimetry

Differential Scanning Calorimetry (DSC) is generally used to measure thermal behavior in material. The conventional DSC involves recording the heat necessary to maintain the same temperature in the sample of interested and the reference material as the two specimens are subjected to an identical temperature range.[13] Whereas, by description, MTDSC uses a modulated temperature profile combined with a deconvolution procedure to obtain the same information as conventional Differential Scanning Calorimetry, as well as the response to the modulation.[17]

MTDSC can be applied to a range of processes governed by Arrhenius type

kinetic behavior and is commonly used for analyzing the weak transitions, complex transitions, initial crystallinity, the heat capacity, and thermal conductivity. The application of MTDSC includes the following types of processes:

1. The irreversible annealing process, crystallization, reorganization, and melting process.
2. The glass transitions.
3. Transformations that follow Arrhenius type kinetics, such as curing, oxidation, degradation, vaporation, etc.

In this research, MTDSC was used to obtain characteristic information over the range of temperatures of the TOF measurements, which is above the glass transition temperature of the systems of interest.

Reference for Chapter 3.0

1. Meyer, Andrew O. Doctoral Dissertation, College of William & Mary, Williamsburg, VA 2001.
2. Mijovic, Jovan and Fitz, Benjamin D. "Dielectric Spectroscopy of Reactive Polymers" Application Note Dielectrics2.
3. Kranbuehl, David E. "Dielectric Monitoring of Polymerization and Cure." In Dielectric Spectroscopy of Polymeric Materials, Runt, J.P., Fitzgerald, J.J., Eds., American Chemical Society, Washington, DC, 11, 1997.
4. Fishbane, P.M., Gasiorowicz, S., Thornton, S.T. Physics for Scientists and Engineers, Prentice-Hall, Inc., New Jersey, 1993.
5. Atkins, P. Physical Chemistry, 5th ed. New York, W.H. Freeman and Company. 1994.
6. Hill, Nora E. "Theoretical Treatment of Permittivity and Loss." In Dielectric Properties and Molecular Behavior, Sugden, T.M., Ed., Van Nostrand reinhold Company, Ltd., New York, 1969.
7. Tipler, P.A. College Physics, Worth Publishers, Inc., New York, 1987.
8. Rogozinski, Jeff Doctoral Dissertation, College of William & Mary, Williamsburg, VA 2000.
9. Jonscher, A.K. Dielectric Relaxation in Solids, Chelsea Dielectrics Press, London, 1983.

10. Chelkowski, A. Dielectric Physics, Elsevier Scientific Publishing Company, New York, 1980.

11. Scaife, B.K.P. Principles of Dielectrics, Oxford University Press, New York, 1989.

12. http://www.ncl.ac.uk/rheology/bsr/frames/define.html.

13. Hood, David K. Doctoral Dissertation, College of William & Mary, Williamsburg, VA.

14. Painter, Paul C., Coleman, Michael M, Fundamentals of Polymers Science, 2nd Edition, Technomic Publishing Co., Inc, Lancaster, Pennsylvania, 1997.

15. Khoshbin, Meisa S. Bachelor Thesis, College of William & Mary, Williamsburg, VA 2001.

16. Argiriadi, M.A. Masters Thesis, College of William & Mary, Williamsburg, VA, 1994.

17. http://www.anasys.co.uk/library/content/DSC/MTDSC.html.

Chapter 4.0

Experimental Procedure

4.1. Measurement Equipment

4.1.1. Time of Flight Measurements

A High-Voltage Source-Current-Measurement unit, Keithley 237, was used to set up the direct voltage and measure the output current. The sensor was immersed in the analyte, and the sensor leads were connected to the Keithley 237. The equipment was operated by and the data stored on an IBM/PS2 computer equipped with data acquisition software developed specifically for this application. After setting relevant experimental parameters, such as voltage, pulse length, and the number of pulses in the setup program, the computer sends the appropriate signal to the Keithley 237, telling the Keithley 237 to put a DC voltage across the sensor electrode. The applied voltage on the electrode attracts the ions and ion migration occurs in the resin liquid, which creates the output current, or rate of ion arrival at the electrode. The Keithley 237 records the output current at time intervals at approximately every 0.33 seconds. There were two types of ovens used to adjust the temperature: Thermolyne 47900 Furnace for the temperatures above room temperature; and a Delta Design 9015 for the temperatures below the ambient temperature. Each oven can be programmed to ramp up or down to a certain temperature, and hold at that temperature for a given

time. To record the exact temperature of materials, a thermocouple was inserted in the resin liquid, out of contact with the sensor. A hand-held device, Barnant Theromcouple Thermometer supplied the real temperature readings. Figure 4.1 shows the experimental setup.

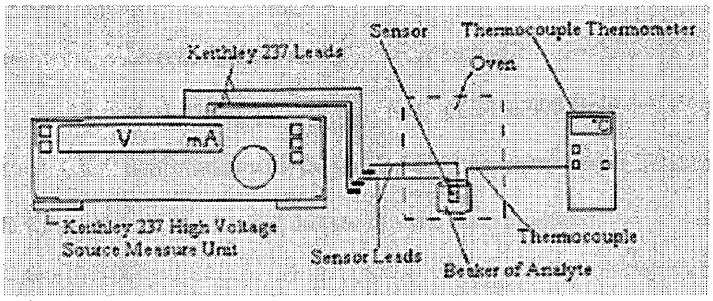

[Figure 4.1] ToF Experimental Setup[1]

4.1.2. FDEMS Measurements

FDEMS measurements was taken by a HP 4192A LF Impedance Analyzer, over a frequency range from 50Hz to 10MHz. A geometry independent interdigitated electrode sensor [Figure 4.2] [2], made of a polyimide Kapton matrix, was used to measure the impedance of the material using the impedance bridge. The impedance measurement system could make multiplexed sensor measurements. The FDEMS sensor is planar, 25 millimeter by 12.5 millimeter in area, and 0.5 millimeter in thickness. Its composition involves a kapton substrate etched with successive layers of conductive metals[2]. The sensor is inert and leads have been attached and epoxy soldering cured at a temperature exceeding 200°C.

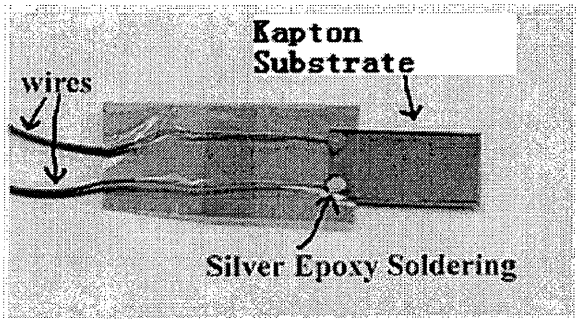

[Figure 4.2] FDEMS Sensor[2]

4.1.3. Rheometry Measurements

Rheometry Measurements were obtained through the Advanced Rheometer 1000 produced by Thermal Analysis Instruments, and used their thermal analysis software. [Figure 4.3] Two types of plates were available for this application: the Peltier Plate and the Parallel Plate. The Peltier Plate, composed of a larger heated plate on the bottom and a smaller oscillating plate on the top, was used in the low temperature range below 100°C. For temperatures higher than 100°C, the Parallel Plate system was used. It uses two identical small size plates on the bottom and top. Using a fixed distance less than one millimeter between two plates, the measurements were taken using the setup parameters: the shear strain, the temperature range, the rate of the temperature ramp, and the frequency sweep of the oscillation.

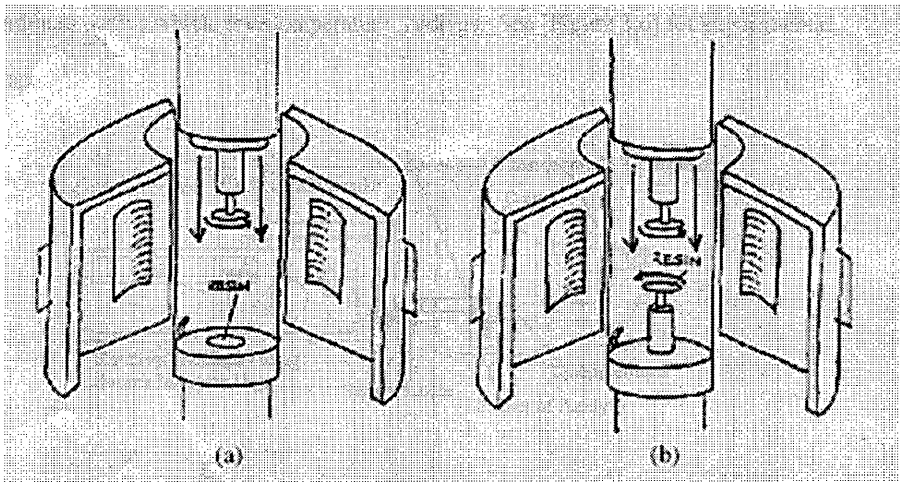

[Figure 4.3] Rheometer Setup (a) Peltier Plate (b) Parallel Plate[1]

4.1.4. DSC Measurements

A Modulated Differential Scanning Calorimeter 2920, produced by Thermal Analysis Instruments, was used to measure the thermal properties of the analyte, namely Tg. The Encapsulate Press device and aluminum hermetic pans were used to prepare the samples for the measurements. The temperature was controlled by the DSC Refrigerated Cooling System. The software provided by the instrument company gave the opportunity to choose the types of temperature modulation. There were three types of choice: Conventional MDSC, MDSC Heat Only, and MDSC Quasi-Isothermal. Since the objective of the DSC is to determine the glass transition temperature of material, Conventional MDSC is precise enough to meet this need. When setting the parameters of the experiments, such as Modulation Temperature Amplitude, Modulation Period, Ramp Rate, fixed values were provided consecutively

as: +/- 1.000°C, 60.00 sec, 1 °C/min. The Tg of six chemicals were initially examined: cyanate, DGEBA, polysulfone, o-terphenyl, MCDEA, and D121. The relative temperature ranges studied were 0°C-150°C, -20°C-100°C, 50°C-300°C, 25°C-200°C, and -70°C-25°C respectively. See [Figure 4.4] for the experimental setup.

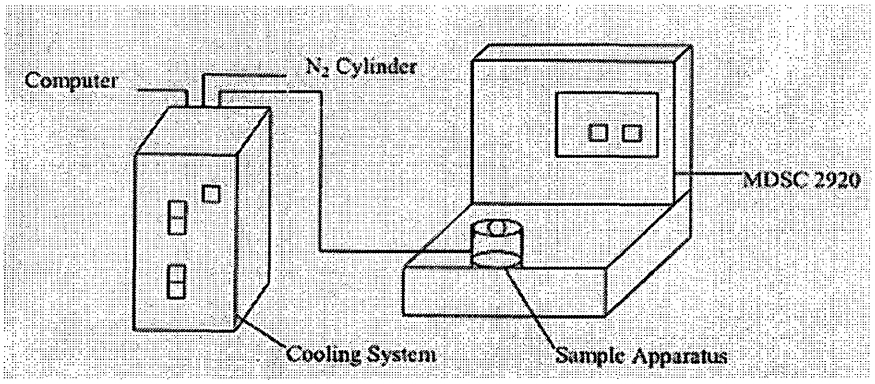

a) Experimental Equipment

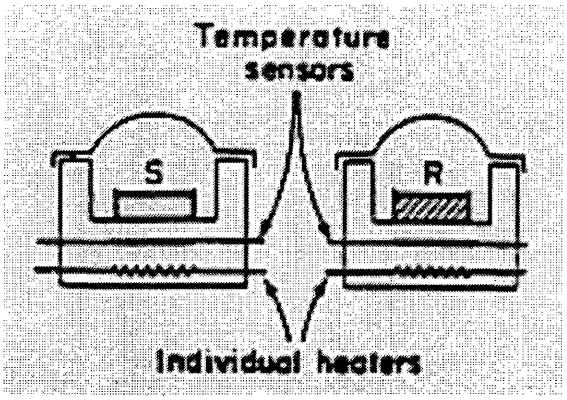

b) Sample Apparatus[3]

[Figure 4.4] DSC Experimental Setup

4.1.5. Chemical Analytes

As mentioned above, six chemicals were examined in this research: 1,1-bis(4-cyanatophenyl) ethane, an epoxy of diglycidylether of bisphenol-A (DGEBA),

polysulfone, o-terphenyl, MCDEA, and a resin of a dimethacrylate monomer (D121). They were selected because we wanted to test materials with a broad range of viscosities without degradation or crystallization, or other changing process. Previous work was carried out on the cyanate resin, a simple, non-hydrogen-bonded system. [Figure 4.5] Due to the high conductivity from the high concentration of ions in this material, a parallel plate capacitor with a large distance between two electrodes was used in the experiments, maximizing the distance for ions to travel. It was found that the time of flight in the cyanate system was too short for real time measurements even with this capacitor. The resin was too fluid and the ion mobility too fast to provide consistent accurate TOF experimental results. The average equilibrium current of the cyanate was approximately 10E-3A in this large capacitor system in a temperature of 30°C to 90°C, again quite high.

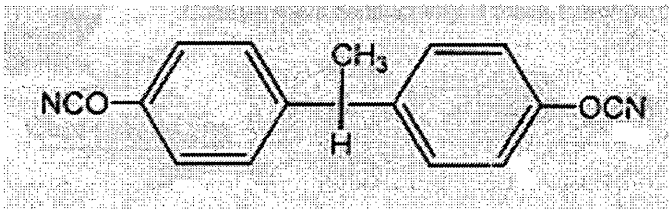

[Figure 4.5] Structure of 1,1-bis(4-cyanatophenyl) ethane

The research was then shifted to other chemicals such as DGEBA [Figure 4.6], polysulfone [Figure 4.7], o-terphenyl [Figure 4.8], MCDEA [Figure 4.9].

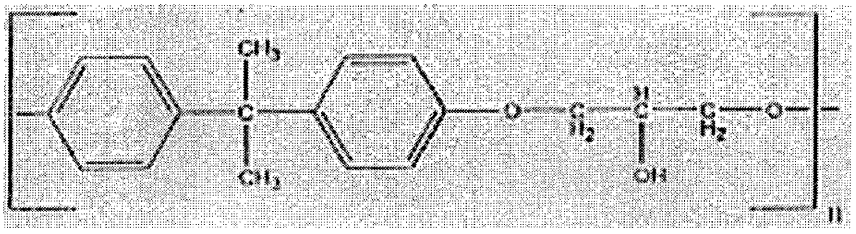

[Figure 4.6] Structure of epoxy of diglycidylether of bisphenol-A (DGEBA)

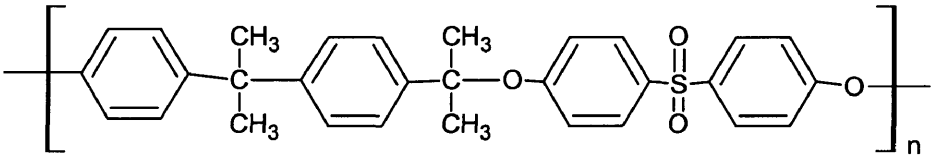

[Figure 4.7] Structure of polysulfone

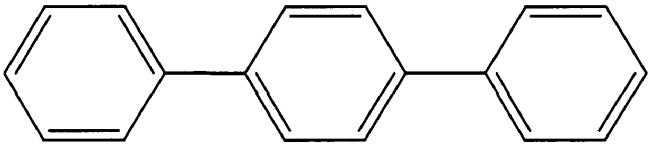

[Figure 4.8] Structure of o-terphenyl

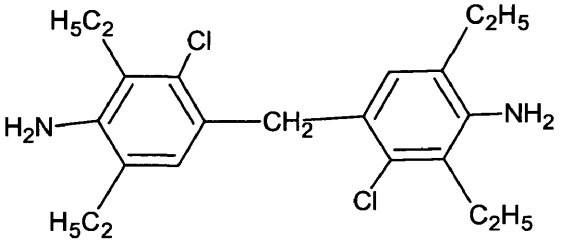

[Figure 4.9] Structure of MCDEA

The DGEBA is relatively viscous medium at room temperature. Because of its hydrogen-bonding properties, it was not an ideal system to study for optimizing the TOF technique. The more viscous medium, polysulfone, was examined next. The polysulfone is supplied as a bead-shaped solid at room temperature. When used in the

experiments, it was necessary to use a high temperature to cast a thin film. The polysulfone film was found to be too viscous to allow for measurable ion mobility, and the conductivity was too low to carry out the TOF experiments. Then o-terphenyl and MCDEA were examined. MCDEA can experience hydrogen bonding, resulting in changes in concentration of changing carriers, and is a complicated place to start when developing a technique. O-terphenyl was a promising system but it did crystallize. The best experimental results occurred when using the simple non-hydrogen-bonded system, dimethacrylate monomer commercially known as D121 [Figure 4.10].

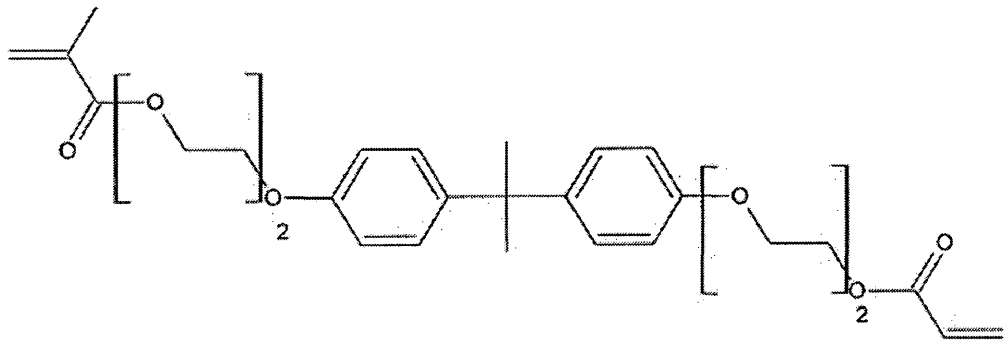

[Figure 4.10] Structure of dimethacrylate of tetaethoxylated bisphenol-A (D121)

4.1.6. Sensor Types

Two interdigitated sensors (one kapton and the other an IDEX sensor) and two parallel plate air capacitors (a small and a large capacitor) were used. The kapton sensor has been introduced in the 4.12 FDEMS Measurements [Figure 4.2]. Three other commercial sensors were used in the TOF technique. The IDEX sensor (036S) consisted of electrodes on a 14" flexible polyimide substrate, with an air gap of 115

microns. The small capacitor (160-110-1) had a large beryllium copper compression rotor contact, and nickel plates, which had a 432-micron air gap. The large capacitor (HFA-25-B) was a single capacitor employing the rotor and stator design, comprised of nickel-plated-phosphor-bronze wiper. The air gap of it was 762 microns. [Table 4.1] described the list of parameters of three geometries. Capacitors were obtained from Cardwell Condenser Corp., and the IDEX from Micromet, Inc.

Sensor Type	Area (cm^2)	Distance(cm)	A/d (cm)
small capacitor	7.86	0.0432	182
large capacitor	21.3	0.0762	280
IDEX	1.04	0.0115	90.2

[Table 4.1] Parameters of Sensors

4.2. Experimental Procedure

4.2.1. TOF Experiments

A number of variables have to be selected before setting up TOF run. Among these are parameters of temperature, sensor type, voltage, and pulse length.

Temperature

DSC experiments were carried out to obtain the thermal properties, mainly Tg, of the different analytes of interest, so that the appropriate temperature range of each material for the TOF experiment could be determined. Theoretically, the temperature range of the measurements should be from slightly above Tg to the temperature where

it is quite fluid in order to examine the system over a range of the viscosity. The following [Table 4.2] shows the data from the DSC experiments.

Matericals	Tg °C	Start Temp °C	Final Temp °C
Cyanate	81.61	30	90
DGEBA	-2.24	25	120
o-terphenyl	-	70	140
polysulfone	181.16	240	265
D121	-45.25	-7	85
MCDEA	-	100	180

[Table 4.2] Tg and TOF Temperature Range

Given the temperature range of chemical analytes, a series of temperature dependent TOF experiments on the different materials were carried out.

Sensor Type

The distances between two electrodes of three sensors are 115, 432, 762 microns respectively for the IDEX, small capacitor, and large capacitor. For the most conductive medium, the cyanate, the longest distance sensor, large capacitor was used. The small capacitor was used with the other five materials because of its appropriate distance for these less conductive materials. The IDEX sensor was also used with the D121 and DGEBA.

Voltage and Pulse Length

Voltage and pulse length are the important parameters in the TOF experiment. They were interdependent with one another. The idealized scheme (Figure 2.2) was

only found to be obtainable under appropriate voltage and pulse length for a given temperature. If the voltage was too low, it was impossible to build up charge migrating across the electrodes. Within the limit of detection, the charge carriers did not have enough time to travel across the relatively long distance. As a result in the experiment, no peak showed up in the current-time plot [Figure 4.11].

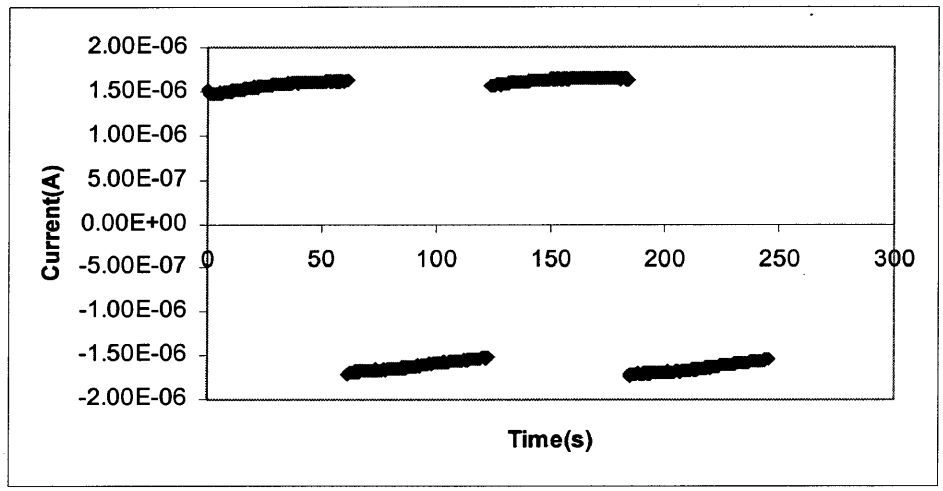

[Figure 4.11] DGEBA: 25C capacitor 60s 400V

Alternatively, if the voltage was too high, two results were observed. One was that the time of fight was too short, from 0.5s to 2s. Such a short time couldn't be accurately monitored, because the instrument took readings at approximately every 0.3s per point. Another factor, the charge polarization at the electrodes was also observed. After the first pulse, a strong reverse pull on the ions was exerted. When the voltage was suddenly switched, an additional time needed to reverse the charge polarization at the electrode, as to release the ions from the electrode. Thus this time was added to standard TOF time factor for the migration of the ions. Double peaks in

the experiment plots were often observed supporting the above explanation [Figure 4.12]. The first peak is potentially the true time of flight, where the second peak marks the arrival of the over polarized ions

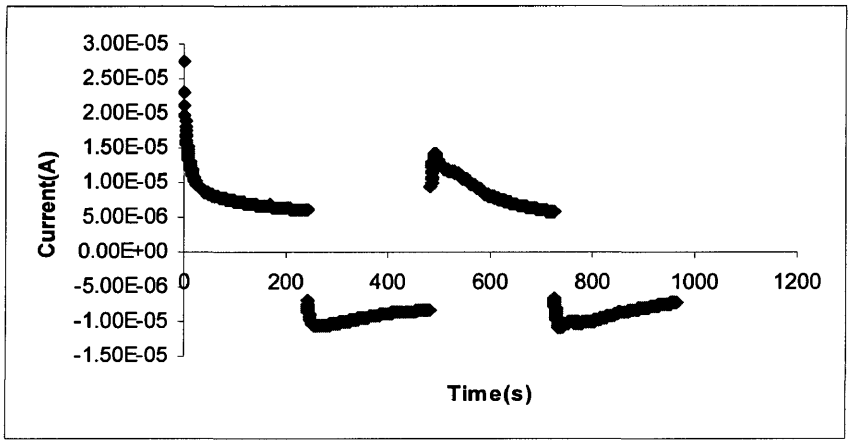

[Figure 4.12] D121: 40C capacitor 240s 400V

The amount of time each voltage was held before the positive and negative electrodes were switched is the pulse length. If the pulse length was too short, the charge carriers did not have enough time to travel across the distance between electrodes. A longer pulse length than necessary would be a waste of time. For the first case, which used a very short pulse length, broad and flat peaks appeared [Figure 4.13].

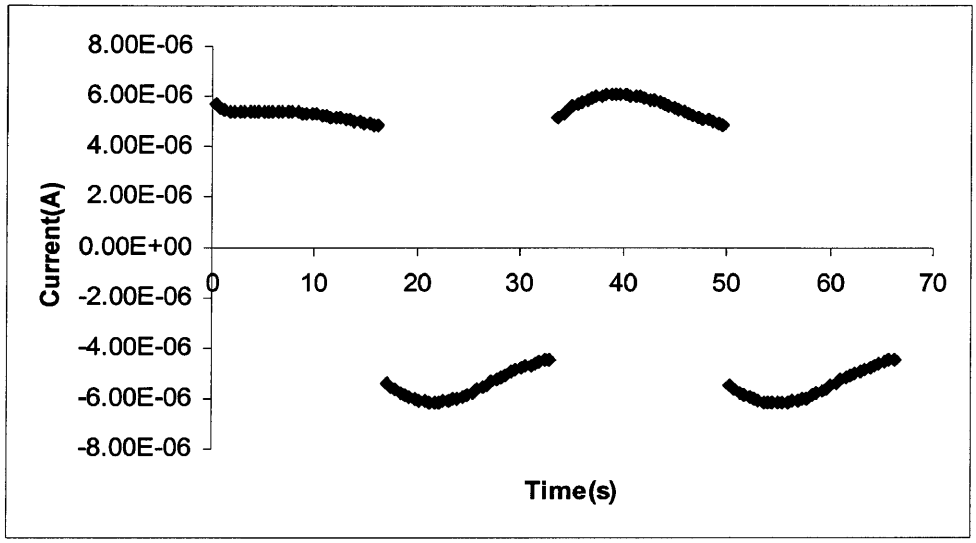

[Figure 4.13] D121: 40C capacitor 15s 50V

But in the case of a very long pulse, an unexpected result occurred. The results were similar to the high voltage case, which showed double peaks [Figure 4.14].

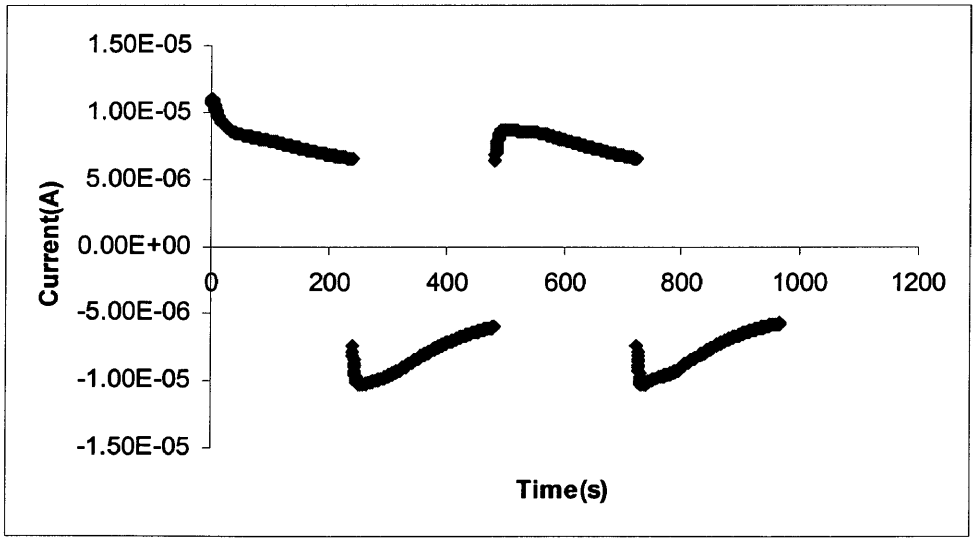

[Figure 4.14] D121: 40C capacitor 240s 200V

An ideal figure of TOF experiment based on the appropriate voltage and pulse length is shown as figure 2.2 (a)(p.9).

Data Analysis

After finishing each run, the data were imported into a Microsoft Excel file. An x-y scatter plot of current vs. time was created and analyzed. The plot showed both the positive and negative pulses of the system. The first pulse was always discarded because the ions would be starting from an equilibrium, non-poled starting position as they did in subsequent pulses. Finding the peak in the pulse, and subtracting the time from the end time of the previous pulse established the time of flight of each pulse. The current was also analyzed in terms for the expected linear behavior according to the voltage. The average start and equilibrium end currents, and the current at the peak of flight were recorded.

Individual Experimental Set-up

The goal of the research was to find the appropriate voltage and pulse length for each material at a particular temperature. Because $TOF*V=d^2/\mu$ (Equation 2.5), and μ is the quantity related to the temperature, the product of TOF and V should be a constant at a fixed temperature and geometry. Thus, there should be a flat range of TOF*V vs. pulse length plot. A series of pulse length dependent experiments were conducted at each temperature. After selecting the right voltage and pulse length, then the temperature was varied. The product of TOF and V being constant at certain temperature was therefore the criterion chosen to determine good experimental data and the correct experimental parameters.

4.2.2. FDEMS Experiments

Typically the electrical conductivity, σ, is obtained through dielectric measurements using an in-situ microsensor and a multi-frequency impedance analyzer. The impedance of a material is measured over a range of frequencies, allowing the determination of capacitance (C) and conductance (G). In this research, FDEMS measurements were compared with the TOF technique.

Specimens for FDEMS cure studies were made by inserting an interdigitated planar sensor into a small beaker filled with liquid material of interested. The FDEMS measurements were collected using a Hewlett Packard impedance bridge controlled with data collecting software. Continuous measurements of capacitance, conductance, and temperature were taken at ten frequencies from 5Hz to $5x10^5$Hz throughout the entire selected temperature range of each material. DGEBA, and D121 were used in FDEMS tests. The real and imaginary components of the complex permittivity were then calculated and recorded for each frequency. The conductivity, σ, of ions in the curing system is a function of the number of charge carriers and the mobility. It is calculated from FDEMS measurements when the product of $\varepsilon''(\omega)$ is constant using the relation $\sigma = \varepsilon_0 \omega \varepsilon''(\omega)$, where ε_0 is the permittivity of free space, 8.85 pF/m, and $\omega=2\pi f$, where f is the measurement frequency.

4.2.3. Rheometry Experiments

Viscosity is related to the temperature. Again viscosity data were obtained for D121 and DGEBA. Both chemicals were characterized using 60mm aluminum plates, and an oscillation procedure, with five frequencies 1Hz, 3.162Hz, 10Hz, 31.62Hz, 100Hz for D121 and 0.1Hz, 0.3162Hz, 1Hz, 3.162Hz, and 10Hz for DGEBA.

Reference for Chapter 4.0

1. Khoshbin, Meisa S. Bachelor Thesis, College of William & Mary, Williamsburg, VA 2001.
2. Rogozinski, Jeff Doctoral Dissertation, College of William & Mary, Williamsburg, VA 2000.
3. McNaughton, J. and Morfimer, C. Differential Scanning Calorimetry, IRS Physical Chemistry Series 2, Butterworths, London, 10, 1975.

Chapter 5.0

Results and Discussions

In addition to Time of Flight, two experimental techniques were used in this research. The FDEMS technique was used to characterize the conductivity. The values of conductivity, σ, measured by the FDEMS technique were compared with those obtained with the TOF technique. Viscosity was obtained through rheology, and is related to the conductivity through equation 2.6 $\sigma = k\eta^{-x}$ and thereby the mobility of TOF.

Rheometry Data

In comparing the DGEBA and D121, one is the hydrogen-bonded material and the other is non-hydrogen-bonded chemical. Two different graphs of the natural log of viscosity (η) versus temperature at lowest frequency measurable were obtained (Figure 5.1 and Figure 5.2).

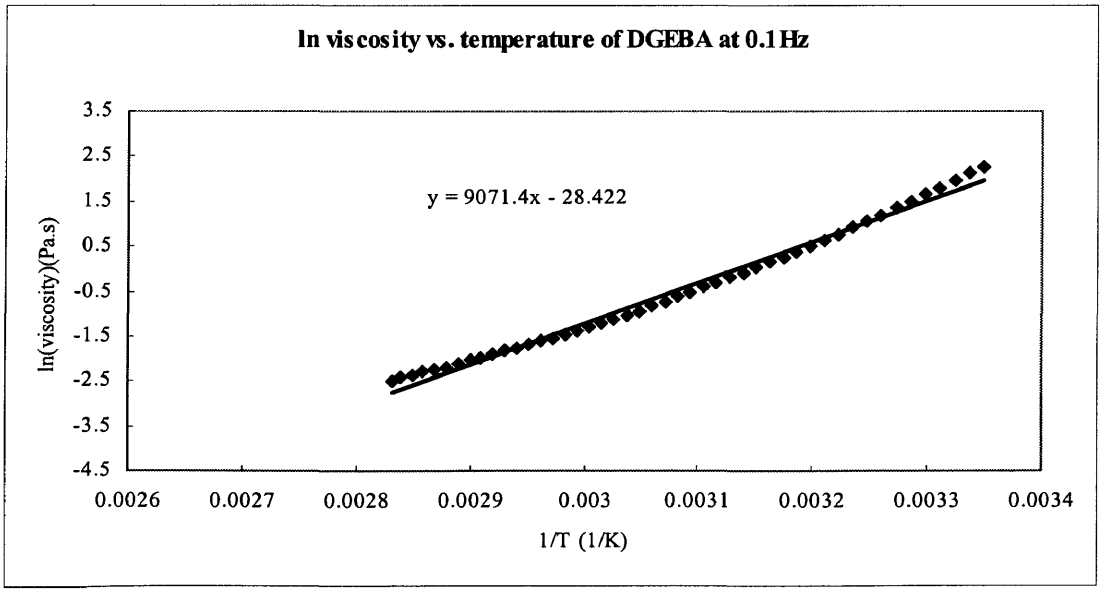

[Figure 5.1] DGEBA ln Viscosity vs. (1/T)

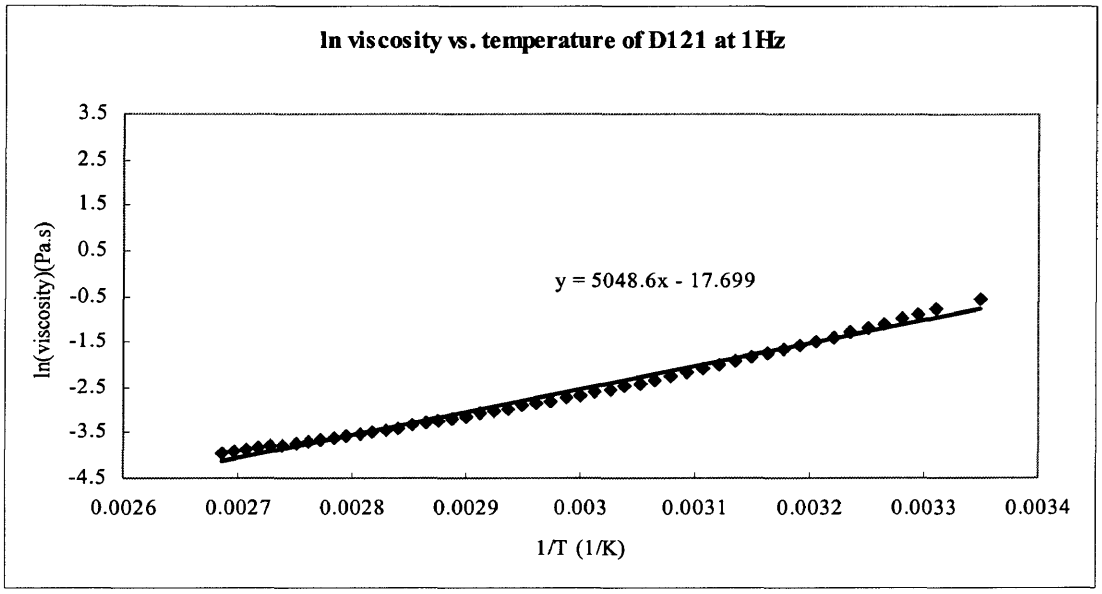

[Figure 5.2] D121 ln Viscosity vs. (1/T)

The viscosities of both materials decrease in an exponential manner as the temperature increases. The equation $\ln(\eta/Pa.s)=9071.4(1/T)-28.422$ fits the data for DGEBA, while for D121 it is $\ln(\eta/Pa.s)=5048.6(1/T)-17699$. Compared to D121, DGEBA is more viscous at a given temperature. But because the viscosity of DGEBA attenuated faster than D121, it is possible to find the temperatures for two maerials at which both materials had the same viscosity. Therefore, DGEBA and D121 could be used as a good contrast in TOF measurement due to their different hydrogen-bonded property but identical viscosity at predetermined temperature.

TOF Data

D121 was an appropriate medium because of its non-reacting and non-hydrogen-bonded character, especially in determining the effect of the

measurement parameters voltage and pulse length on the TOF technique. As a result, most of the experimental data were obtained and discussed based on D121 experiments. DGEBA is one of the simplest materials of epoxy group, which are the prevalent materials to be applied in industries. Thus DGEBA was also used but was of less importance due to its hydrogen-bonded property.

Pulse length together with magnitude of applied voltage was examined. First, pulse length dependent data were analyzed at a fixed temperature of 40°C. An interdigitated (IDEX) sensor system and a parallel plate air capacitor (small capacitor) system were used to acquire the data. To see the effect of varying pulse length, the log of TOF*V versus the pulse length for each type of sensor was plotted for different voltages. Because TOF = $d^2/ \mu V$ (Equation 2.5), the product of TOF and V is the quantity which monitors the ion mobility μ for a fixed distance between plates of the sensor. When the experimental results are consistent with equation 2.5 at a fixed temperature, the product of TOF and voltage will be constant. The plots for both sensor systems display many points scattered around a fixed value. There are two reasons for this scatter. If the pulse length is too small and/or the voltage is too weak, ions migrate only partially to the opposite plate. That is the major concentration of charge is between the two plates. When the voltage is reversed on the electrodes, the shorter distance for the major concentration of ions to travel produces a smaller value for the TOF. If the voltage is too strong and/or the pulse length is too long, a polarizing process can be created. When the voltage is reversed on the electrodes, an

additional time is needed to reserve the excess charge polarization effect and pull the ions from plates. As a result, one observes a longer TOF.

Next we examined the effect of distance between the electrodes by comparing the two sensors with different electrode space. For (Figure 5.3) with an IDEX sensor, a line has been drawn through those experimental points. The points were chosen based on the fact that the product of TOF*V should be independent on the voltage at each pulse length. Thus the product of TOF and voltage is a constant. The value of log(TOF*V) for this line is approximately 2.0.

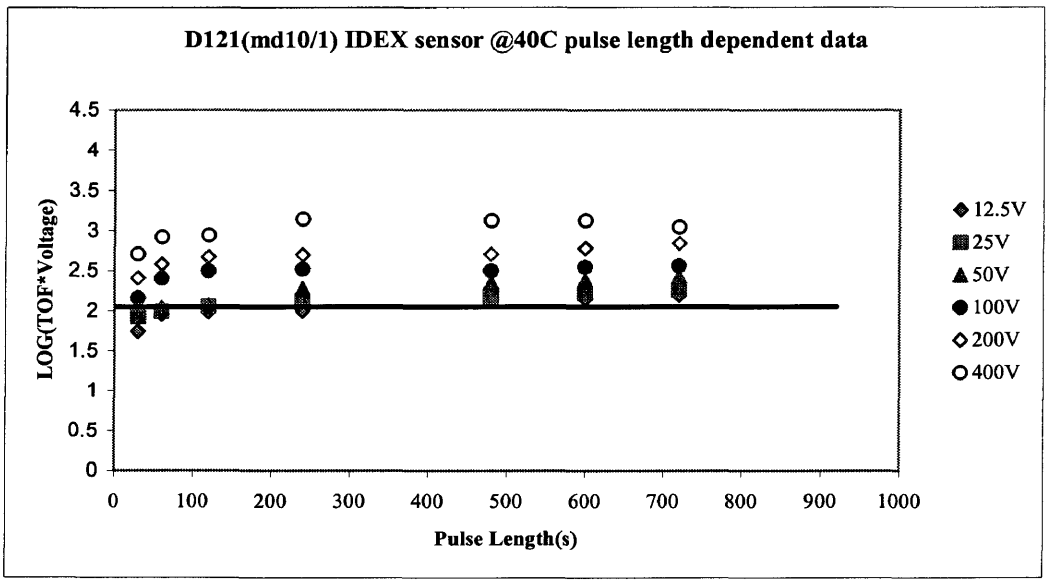

[Figure 5.3] D121 IDEX Sensor @40C Pulse Length Dependent Data

Many points are above that value due to too strong a voltage in the small distance IDEX geometry sensor. Only at a short pulse length (30s) and low voltages (12.5V) are the experimental points below that line. When the pulse length increases

to a very large value, even at these lower voltages, the points fall above the constant value and scatter as well. In the case of the small capacitor (Figure 5.4), the constant value of log of TOF*V is 3.1.

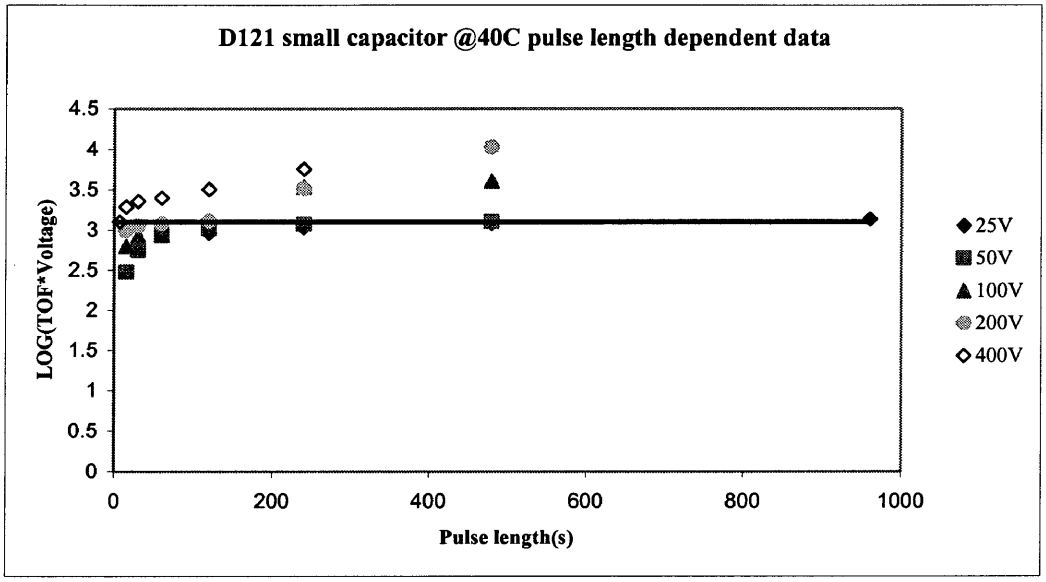

[Figure 5.4] D121 Small Capacitor @40C Pulse Length Dependent Data

Compared to (Figure 5.3), more points are below the linear value. These occur at short pulse lengths (<120s) and lower voltages (25V and 50V), because the small capacitor has a relatively larger distance of 4.3E-06m between the electrodes. This is to be compared to 1.2E-06m between the electrodes of the IDEX sensor. Therefore, a longer pulse length is needed to pull all the ions across the distance of the electrodes and to build up enough charges at the electrodes to an ideal level for accurate TOF measurements. Thus, the sensor's electrode space plays an important role in the ion mobility measurement. Different sensors will have a different distance between two

electrode plates, and thereby a different range of voltages and pulse lengths that produce good TOF results. The ratio of the small capacitor electrode separation to the IDEX sensor electrode separation is 3.6, and the ratio $d^2=(3.6)^2$ is 13.0. The constant values of log of TOF*V of the small capacitor and the IDEX sensor are 3.1 and 2.0. The ion mobility μ is constant at the same temperature. Thus, the experimental ratio of TOF*V for the two geometries is 12.6, which is close to the theoretically predicted ratio of 13.0 based on the two distances. This result shows that the ion mobility does not change with geometry, and again is in agreement with (Equation 2.5). It also shows that both of these sensor systems provide good Time of Flight results.

Next we compare the TOF responses of D121 and DGEBA as a function of temperature. The log of TOF*Voltage versus temperature for the small capacitor with D121 and DGEBA are plotted [Figure 5.5] and [Figure 5.6]. All the experimental points are included.

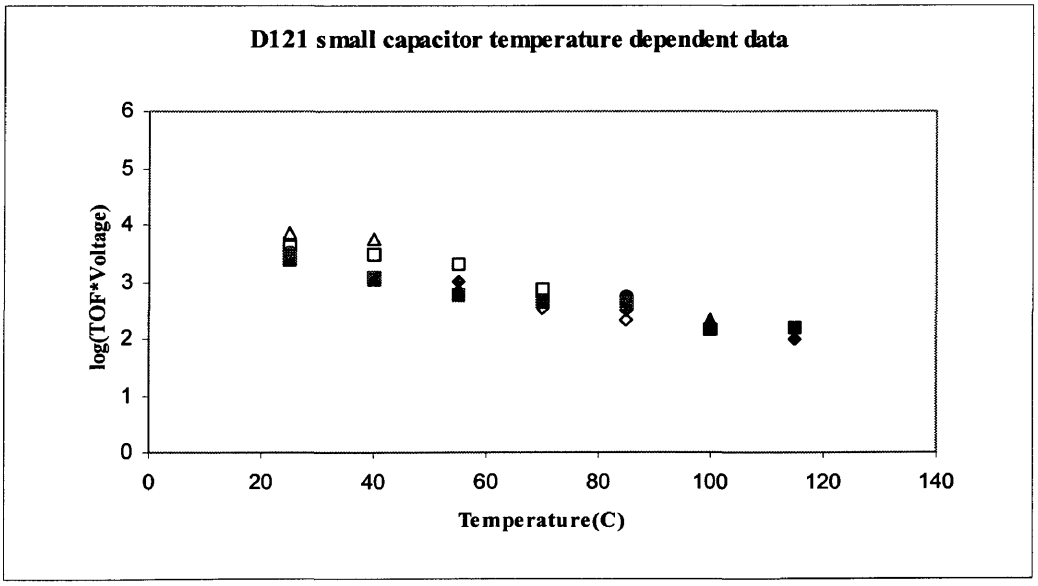

[Figure 5.5] D121 Small Capacitor Temperature Dependent Data

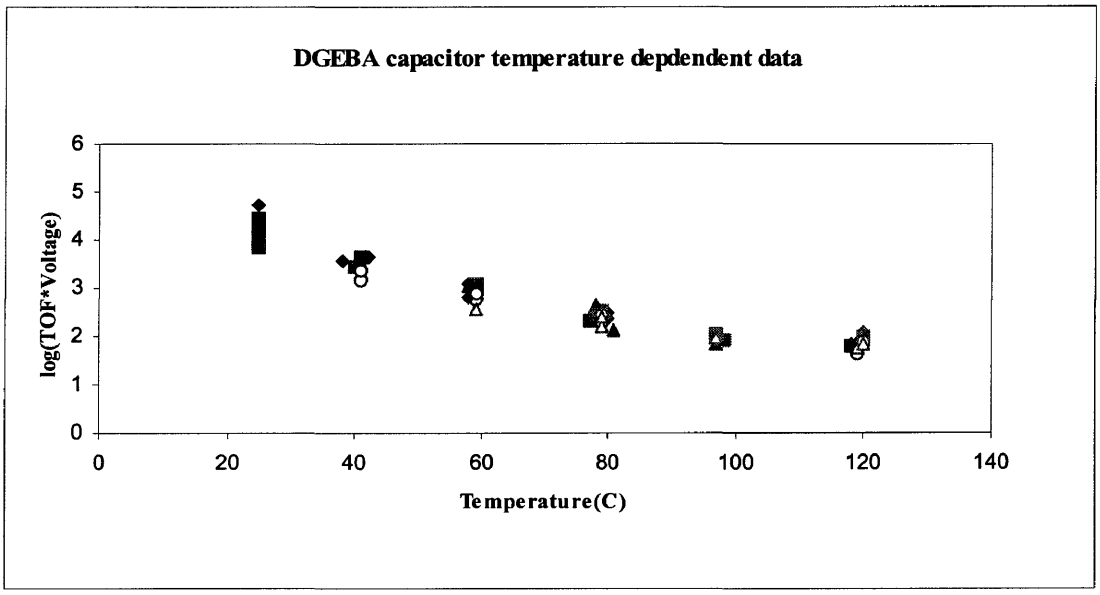

[Figure 5.6] DGEBA Small Capacitor Temperature Dependent Data

Comparing log(TOF*Voltage) versus temperature plots of D121 and DGEBA, the same trends are apparent. The product of TOF and voltage is a function of temperature. As shown in (Equation 2.5), the ionic mobility is also a function of temperature. From the viscosity data of the two chemicals, we observe that the viscosity of D121 at 25°C is the same value of 0.6 as that of DGEBA at 55°C. The average value of log(TOF*Voltage) for D121 at room temperature is approximately 3.7 compared to the value of 3.0 for DGEBA at 55°C. Since the product of TOF and voltage has the inverse ratio to the mobility, D121 has a relatively small ionic mobility compared to DGEBA. Thus one reason that the hydrogen-bonded system has a rather large conductivity is that the ionic mobility due to proton exchange is faster than diffusion of ions in the non-hydrogen-bonded media.

The slope of the linear best-fit product of log(TOF*Voltage) versus temperature

for DGEBA is larger than that for D121. This can be explained in that temperature decreases the viscosity move in the hydrogen bonding system of DGEBA.

FDEMS Data

As described in FDEMS experiments, the electrical conductivity of a material is derived from (Equation 3.24) $\sigma = \omega\ \varepsilon_0\ \varepsilon''$, where σ is a constant over a range of frequencies.

But in the TOF technique, the electrical conductivity of a material is defined as the current flowing through the material under a static electrical potential,

$$\sigma = Id / AV$$

[Equation 5.1] [1]

where I is the equilibrium current at the end, d is the distance between the electrodes in centimeters, A is the area of the electrode plate in cm^2, and V is the voltage of the TOF measurement.

Figure 5.7 shows the experimental conductivity from TOF and FDEMS measurements.

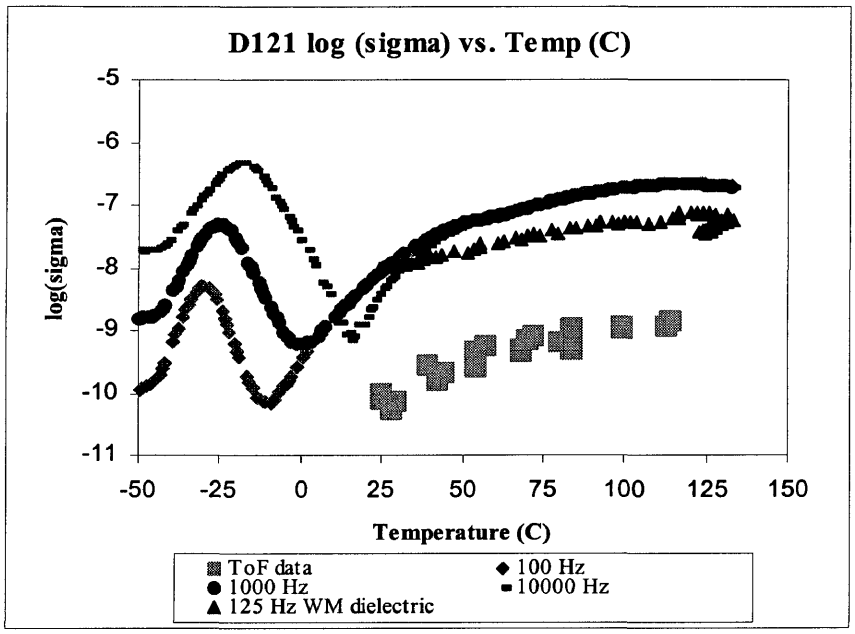

[Figure 5.7] D121 TOF and FDEMS Sigma versus Temperature

The conductivity data of both the techniques has the same trend with increasing temperature. Thus TOF and FDEMS results differ in magnitude but show the same dependence on temperature. The reason for the difference can be explained in that the TOF technique has the charge polarization effect. Extra charges have been built up at the electrodes during the experiment. This results in the lower conductivity calculated from TOF than the measurable conductivity from FDEMS.

Compiled Data

Since the ionic concentration, N*i* is constant in the non-hydrogen-bonded D121, the product of TOF, voltage, and conductivity should return a constant value regardless of temperature. Note TOF = $d^2/ \mu V$ (Equation 2.5), and the relationship of

σ and μ through the equation σ/μ=N in the case where N is a constant. Combining the two equations, we get (σ*V*TOF)=N for all magnitudes of voltage given a constant geometry. This quantity is plotted versus temperature for D121 (Figure 5.8).

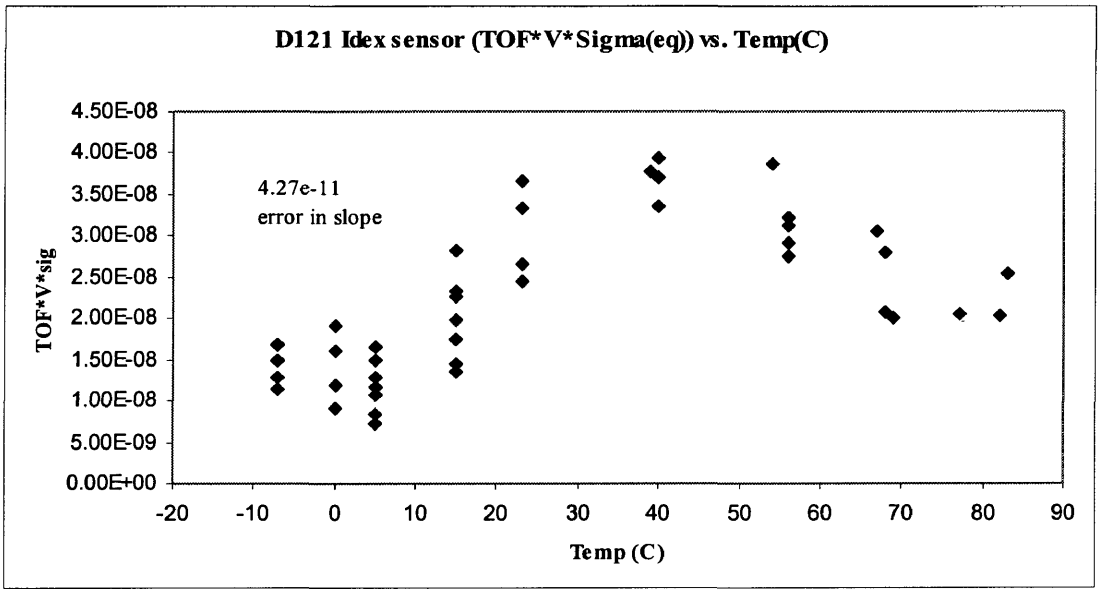

[Figrue 5.8] D121 IDEX Sensor (TOF*V*Sigma) vs. Temp

There is an inherent scatter in the value. The lack of trend in the data shows that the value of N*i* is not increasing or decreasing in a discernable trend. The scatter indicates the range of error associated with the TOF measurement.

Figure 5.9 shows that for DGEBA there is also no detectable change or trend in the number of charge carriers with temperature. Compared to D121, DGEBA has a bigger value in the number of charge carriers and a bigger range of scatter.

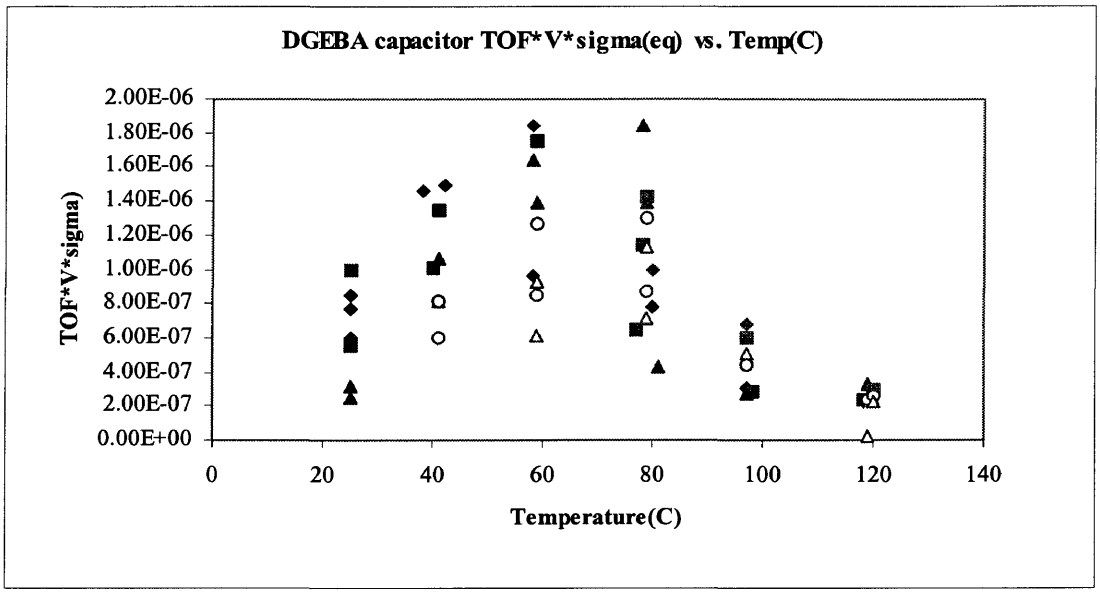

[Figure 5.9] DGEBA small Capacitor (TOF*V*Sigma) vs. Temp

Considering the challenges inherent in in-situ monitoring during cure, one of the goals of this research is to explore the application of the technique during polymerization. At the onset of the research, we tried to validate the relationship of the conductivity, mobility and viscosity by the equations of $\sigma = k\eta^{-x}$ and $TOF*V = d^2/\mu$. Since the quantities of conductivity, TOF*V, and viscosity are all functions of temperature, the conductivity and TOF*V were plotted versus viscosity directly. [Figure 5.10]

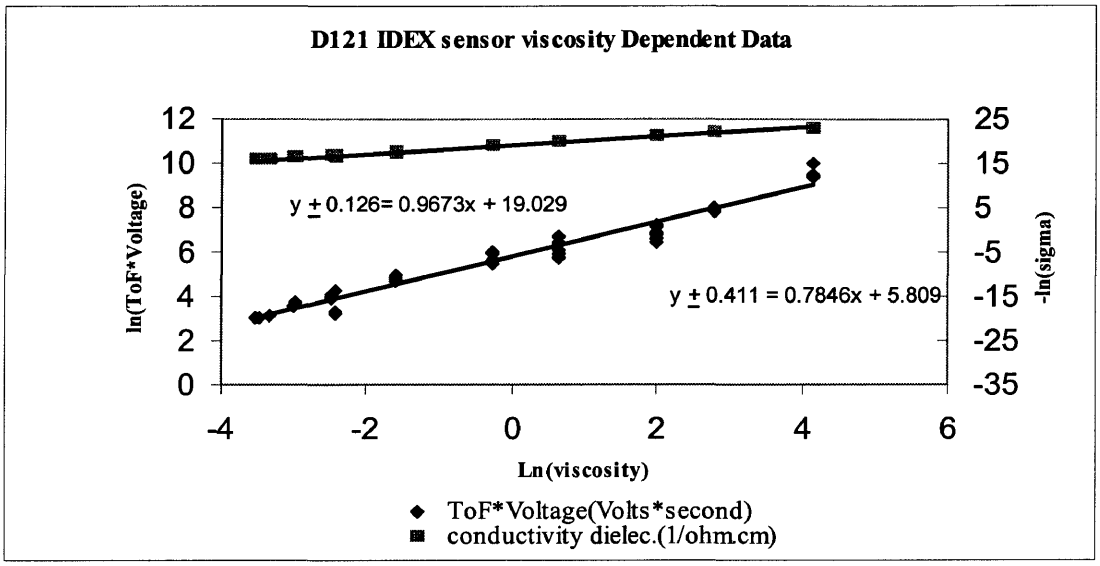

[Figure 5.10] D121 IDEX Sensor Viscosity Dependent Data

The above plot demonstrates that the conductivity, determined through dielectric measurement, is directly proportional to the viscosity, and the experimental value of x is 0.97. The value of TOF*V versus viscosity has a slightly lower slope. The difference is probably due to variation in the materials, such as moisture-humidity and particularly experimental uncertainty in the measurements.

In this research, the objective to determine the measurement parameters for the TOF technique has been achieved, and the ability to analyze the data has been shown. These were accomplished through optimizing parameters of voltage, and the pulse length for a material of interest at different temperatures, and plotting the value of TOF*Voltage versus pulse length to obtain valid data. Future work will focus on hydrogen-bonded systems, which experience an increasing and variable number of mobile species, as the number of hydrogen bonding groups change.

References of Chapter 5.0

1. Seanor, Donald A. "Electrical Conduction in Polymers." In Electrical Properties of Polymers, Academic Press, Inc, New York, 1982.

Chapter 6.0

Conclusions

The initial goal of this research was achieved to determine the correct measurement parameters for the TOF technique. The ability to analyze the data and monitor the mobility has also been shown. The following is a summary of specific conclusions.

Viscosity affects the conductivity of the materials of interest. The conductivity is a function of ionic mobility and the number of ionic species. The viscosity is related to the temperature. Therefore the temperature is the first parameter, which should be considered.

The TOF technique measures the transit time (time-of-flight time) of ions traveling across the electrodes. The distance of the electrodes has a direct influence upon the magnitude of transit time. The TOF instrument, Keithley 237, records the output current at time intervals of approximately 0.33 seconds per point. Considering the experimental errors, a "good" time-of-flight time should be no less than 5s and the electrode space of the sensor needs to be selected to achieve this result.

Pulse length and voltage need to be carefully selected. The theoretical prediction of TOF*V equals a constant and is the criteria to choose the voltage and pulse length. Thus at each temperature, a plot of TOF*Voltage versus pulse length should be made. The product of TOF and voltage should be constant for accurate measurements of TOF. This is shown by the linear values on the plot.

No time is needed to short the electrode circuit between pulses. Any build up of charge that may occur at an electrode is inconsequential to any subsequent runs.[1]

Time of Flight measurement is an appropriate technique to separately monitor the ionic mobility. In the D121 system, at fixed temperature, we used two different sensors, a small capacitor and an IDEX sensor, to demonstrate the credibility of the equation $TOF = d^2/ \mu V$. Then in the same geometry, and with the same viscosity, we demonstrated that the DGEBA has a relatively higher mobility than the D121, due to its hydrogen bonding property.

Additionally, Time of Flight is a potential technique to accurately and on-line measure the macroscopic viscosity of a polymer during the curing process. A proportionality relationship in the D121 system is obtained as

$$TOF*V \propto 1/\mu \propto \eta^{0.78}$$

where μ is the mobility of ions, and η is the viscosity.

Coupled with FDEMS measurement, TOF technique is able to monitor the change in the number of charge carriers. Time of Flight technique measures the mobility of ions, while FDEMS technique measures the ionic conductivity. Through the equation $\sigma = \sum N_i \mu_i$, it is possible to determine the variable in ion concentration. Future work will focus on the hydrogen-bonded systems.

Reference for Chapter 6.0

1. Khoshbin, Meisa S. Bachelor Thesis, College of William & Mary, Williamsburg, VA 2001.

VITA

Jie Guo

Born in Gansu, P.R. China, June 20, 1971. Graduated from No. 1 Middle School of Fuzhou, July 1990. Earned a Bachelor of Science with a concentration in Chemistry from Fudan University, Shanghai, July 1995. From August 1995 to February 2000, worked as an Analytical Chemist in Fuzhou Environmental Monitoring Institution.

In August 2000, became a graduate student for Master of Arts study in the Department of Chemistry at the College of William and Mary.

Upon graduation the author plans on attending the University of Maryland at College Park to pursue a Doctorate in Organic Chemistry.